ISSN 1330-9862
(FTB-2249)

original scientific paper

Morphological and Structural Characteristics of Zein Biofilms with Added Xanthan Gum

Crislene Barbosa de Almeida[1], *Kelly Tafari Catelam*[1], *Marinônio Lopes Cornélio*[2] *and José Francisco Lopes Filho*[1]*

[1]Department of Food Engineering and Technology, UNESP, São Paulo State University, R. Cristóvão Colombo 2265, CEP 15054-000, São José do Rio Preto, Brazil

[2]Physics Department, UNESP, São Paulo State University, R. Cristóvão Colombo 2265, CEP 15054-000, São José do Rio Preto, Brazil

Received: March 3, 2009
Accepted: October 1, 2009

Summary

Morphological and structural characteristics of zein-based biofilms have been studied in this work. The sorbitan component in the control formulation of the film was substituted with xanthan gum at concentrations between 0.01 and 0.04 % to analyze its effect on lipid dispersion. Scanning electron microscopy (SEM) showed a surface for the control (0 % xanthan) with good lipid distribution. However, when the samples were investigated by optical microscopy (OM), lipid globules in the control biofilm appeared larger and more dispersed in the matrix than in the other samples. Fourier transform infrared (FTIR) spectroscopy indicated that xanthan concentrations deeply affected C=O linkages from amide I group, as well as the functional N-H group of amide II of the zein structure. Other weak interactions of amide I and II with carboxylic acids and aliphatic compounds were also observed. UV/VIS analysis as well as transparency measurements indicated that the addition of xanthan to the film matrix lowered significantly its transparency properties. Overall, the addition of xanthan gum favoured lipid dispersion in the matrix, making biofilms more homogeneous, although less transparent.

Key words: zein biofilms, xanthan gum, morphological properties, structural properties

Introduction

Since the 1980s, edible films have been of great interest to the food industry as carriers of nutrients and as biodegradable films (*1*). Natural biopolymers, polysaccharide- and protein-based, show the highest potential, mainly because they are renewable, abundant, economic to produce and can form a continuous matrix.

Zein, the main alcohol-soluble corn protein, is commercially produced from corn gluten, a coproduct of the corn wet milling process. This protein has low biological value due to amino acid imbalance: high content of leucine and glutamine and low content of lysine and tryptophan (*2–4*). A major advantage of zein, as compared to other corn proteins, is its polymerization property. It has twice more potential than necessary to produce linear polyamide/polyester polymers (*5*).

Microbial biopolymers are polysaccharides produced by different types of bacteria, fungi and yeast. These materials have the capacity of forming gels and viscous solutions even at low concentrations (*6*). They are also important due to their emulsification properties, crystallization control, syneresis inhibition, encapsulation, and film-forming capacity (*7*). Among these biopolymers, xanthan has been used in several food preparations. According to Morris (*8*), xanthan or xanthan gum is an important food additive due to its functional properties as well as the improvement in several food characteristics.

*Corresponding author; Phone: ++55 17 32 212 254; Fax: ++55 17 32 212 299; E-mail: lopes@ibilce.unesp.br

Xanthan is a natural polymer, hydrophilic, produced through sugar fermentation by microorganisms of the gender *Xanthomonas campestris* (*9*). The main reason for the addition of xanthan to the filmogenic solution was to verify if its characteristics could improve the film functionality.

According to Lai and Padua (*10*), zein biofilms show good transparency. When plasticizers are added to the matrix, the material becomes more flexible, although some properties can be modified as, for example, increasing opacity (*11,12*). In order to improve the material characteristics, co-polymerization and different polymeric blends have been produced and characterized (*13*).

During polymeric material development, a physical mixture of two or more polymers forming a polymeric blend attracted, most of the time, more attention than polymer synthesis. This happened mainly because the combination of polymer properties resulted in materials with different properties that are often better than the individual polymer properties. This process is easier and less expensive than the investigation of new synthetic route. The properties of final polymeric blend depend on the miscibility of the constituents or the morphological structure of each phase in the case of heterogeneous blends (*14*).

For understanding polymer-polymer miscibility, scanning electron microscopy (SEM) and Fourier transform infrared spectroscopy (FTIR), among other techniques, have been used (*15*). Material incorporation in the matrix can form a homogeneous or heterogeneous structure depending on their interactions. Optical microscopy (OM) and SEM allow the identification of the material incorporated in the matrix and permit its characterization through the observation of colour and shape.

Other less conventional methods like photoacoustic spectroscopy (PAS) are used, in some cases, to complement usual transmission techniques. These techniques allow a more complete understanding of the material using the properties of transparency and/or heat capacity to characterize the product. The PAS technique uses acoustic signal detection generated by a sample through modulated radiation. The sample is placed in a small chamber with a high definition microphone. Intensity modulated radiation is applied on the sample and the absorbed radiation spectrum is computed (*16*). The spectroscopy of generalized bidimentional correlation is a technique of simple correlation that permits the access to information not easily visualized with unidimensional spectra. Their spectrum can be analyzed through surface maps, which facilitates the comprehension of the observations (*17*).

The transparency/opacity of the material shows its capacity to block the light. Low transparency or high opacity indicates that the material is a good light blocker. Biofilms used as packing or food covering should have high transparency when the characteristics of the packed product have to be visible (*18*).

The aim of this research is to produce biofilms based on zein with added sorbitan or xanthan gum at different xanthan concentrations, and to determine their morphological and structural characteristics. SEM, OM, FTIR, PAS and transparency/opacity determinations were used to characterize the biofilms.

Materials and Methods

For each treatment, zein-based materials were prepared according to Kleen *et al.* (*19*), with some adaptations, by dissolving granular zein in a 75 % aqueous ethanol to a concentration of 16 % (by mass per volume) at room temperature. Oleic acid was added at a ratio of 70 g per 100 g of zein, while stirring the solution on a water bath at 60 to 65 °C. Glycerol was added at a ratio of 30 g per 100 g of zein and 0.01 % of sorbitan or four concentrations of xanthan were added. Xanthan concentrations (by mass per volume) were 0.01, 0.02, 0.03 and 0.04 %, related to the total material. The filmogenic solution was stirred mechanically for 10 min and submitted to 20 mHz of ultrasonic frequency (Fisher Scientific®) for another 10 min, after which it was cast on rectangular acrylic plates and maintained at room temperature (25 °C) for 48 h to dry. After drying, the formed films were peeled off and stored inside the desiccator at 58 % relative humidity until analyses.

The thickness of films was determined by the arithmetic mean of six values measured in six randomized points of each sample using a digital micrometer with 0.001 mm resolution (Digimess, Brazil), and the average thickness was (0.12±0.03) mm.

SEM is a common technique for analyzing the microstructure of biodegradable films. This technique has been used for decades to study the global structure of proteins, mainly quaternary conformations (*20*). For this analysis, film samples of 12 mm in diameter were fixed on stubs with double-sided tape with conductive copper and covered with 35 nm of gold (Emitech K550, UK). Samples, taken in duplicate, were observed under an electronic microscope (LEO 435 VP, UK) at 15 kV in a climatized room.

Optical microscopy was used to identify the formed compounds in films stained with Xylidine Ponceau (pH=3.5), which permits the detection of cationic protein radicals (*21*). Periodic acid-Schiff stain was used to identify neutral polysaccharides and glycoproteins (*22*). The samples, taken in duplicate, were stained directly without previous fixation and dehydration because of the zein solubility in alcohol solutions, which are used to fix the material. Instead of the fixation by the ethanol-based solution, the glass slides (microscope laminae) were dried in an oven (Odontobras ECB 1.2 Digital, Brazil) at 37 °C for 24 h and mounted with Canada balsam. After 24 h, the samples were analyzed at room temperature using an optical microscope (Olympus BX 60) with an image capture system (Olympus DP 71). Different points in the sample were observed with 10× magnification.

Fourier transform infrared spectroscopy with attenuated total reflectance accessory (FTIR-ATR) was used as complementary analysis. The infrared spectra were acquired by using a Spectrometer Nicolet Nexus 670 FT-IR ESP. Samples of 7×70 mm were fixed in the ATR and the spectra were recorded in the range from 4000 to 1200 cm^{-1}, with a resolution of 4 cm^{-1} and 128 scans. This range was used because it encloses amide I and II bands, which are the main portions for protein characterization (*23*).

The photoacoustic spectroscopy (PAS) data were collected with homemade equipment assembled in the Physics Laboratory of UNESP, São José do Rio Preto, Brasil. The determinations were performed placing the samples in a transparent acrylic support and the readings were done in the UV/VIS range from 200 to 600 nm. Photoacoustic chamber consisted of a steel cylindrical cell with a quartz window and a high sensibility microphone (*24*).

Film apparent transparency was determined with a UV/VIS spectrophotometer (Quimis, Brazil), as proposed by Gounga *et al.* (*25*). Samples of rectangular shape were applied to the internal wall of the cuvette. Three replications were done for each film at 600 nm. Film transparency was calculated by dividing the absorbance at 600 nm with the film thickness.

Analysis of variance (ANOVA) was performed considering a randomized experimental design and Tukey's test applied to compare data means at 5 % probability using a computational program ESTAT, v. 2.0, according to Banzatto and Kronka (*26*).

Results and Discussion

The homogeneity of the samples was observed by electron micrographs and it is shown in Fig. 1, where it can be observed that an increase in xanthan concentration promotes changes in the surface of the material, interfering with the distribution of compounds. The control (Fig. 1a) presented the best distribution of fat globules, which is identified by the black points in the picture. Apparently, there was no formation of a continuous layer of the matrix in the other films with various xanthan concentrations. Similar observations of black points on the material surface were found for zein biofilms in the work done by Corradini (*27*) and Ghanbarzadeh *et al.* (*28*). The first insight suggests that these points are microbubbles entrapped inside the matrix or spaces occupied by glycerol before the drying process (*25*). However, there is a possibility of phase separation between zein and glycerol due to the low interaction between these two compounds (*27*).

During biofilm formation, difficulties in homogenizing the solution were observed as xanthan concentrations increased, manly 0.03 or 0.04 %, when some lumps appeared as spots in the film. In order to better characterize these lumps, as well as the points found on the surface, optical microscopy was performed to observe the homogeneity through distribution of protein and fat globules.

Figs. 2 and 3 show the images magnified ten times (500 μm) obtained for each xanthan concentration using two kinds of sample preparation: Xylidine Ponceau (pH=2.5) and periodic acid-Schiff staining. The red colour represents protein fraction and the white points the fat globules (Fig. 2). As xanthan concentration increases, the size of fat globules decreases, enhancing better homogenization of the material into the film matrix (Fig. 3). It can be observed that increasing xanthan concentration resulted in bluer colour of the sample. Fig. 3d (0.04 % xanthan) shows lower amount of dispersed fat globules, confirming the observations shown in Fig. 2 (Xylidine Ponceau staining).

The control sample also presents a slightly purple colour, which indicates that the periodic acid-Schiff reagent stained the hydroxyl radicals of the matrix structure (*29*).

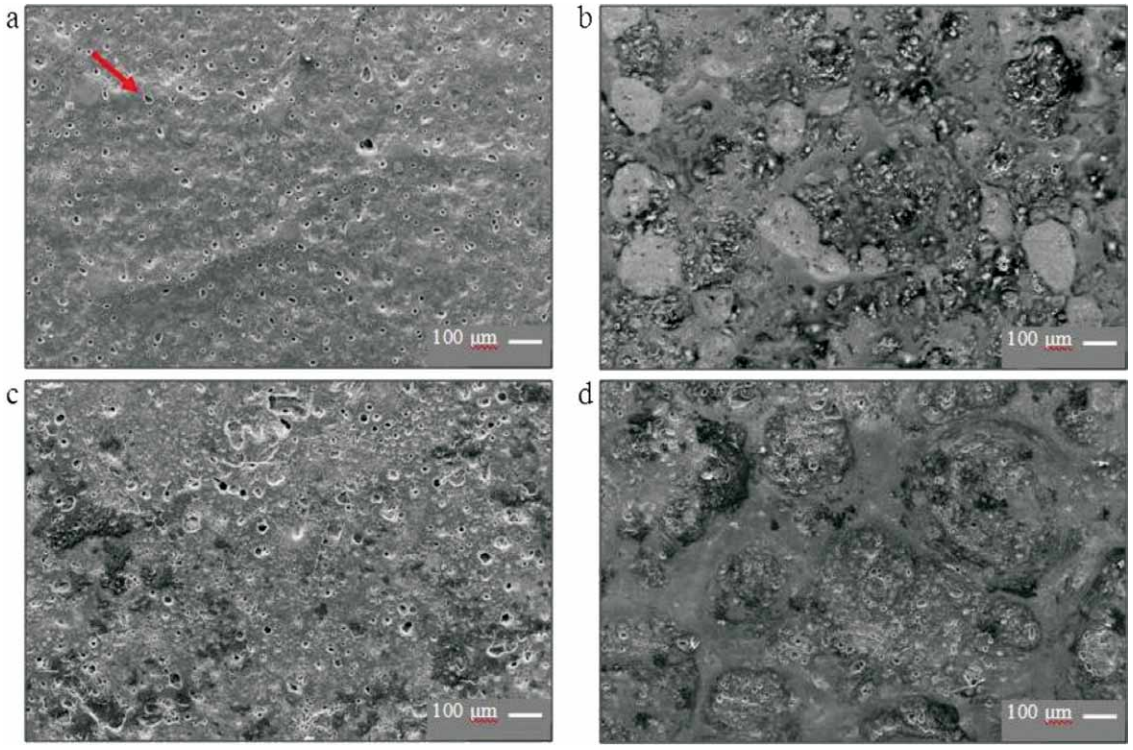

Fig. 1. Scanning electron micrographs of zein-xanthan biofilms. *w*(xanthan)/%: a) 0 (control), b) 0.01, c) 0.02, and d) 0.04

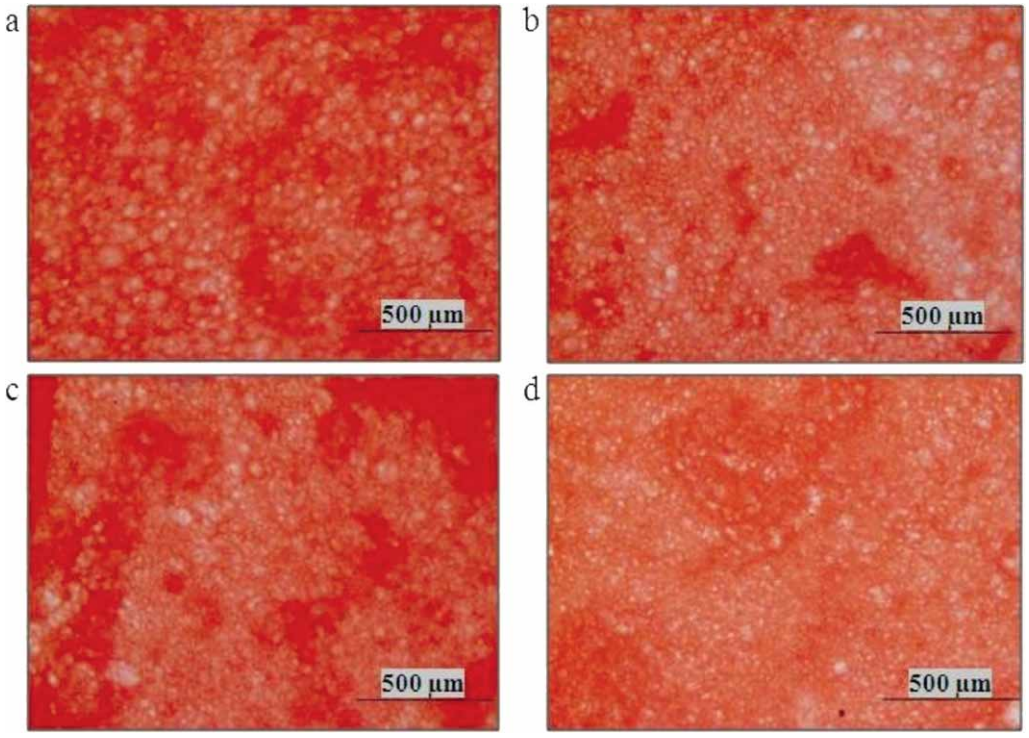

Fig. 2. Optical microscopy with Xylidine Ponceau (pH=2.5) stain for zein-xanthan biofilms. *w*(xanthan)/%: a) 0 (control), b) 0.01, c) 0.03, and d) 0.04

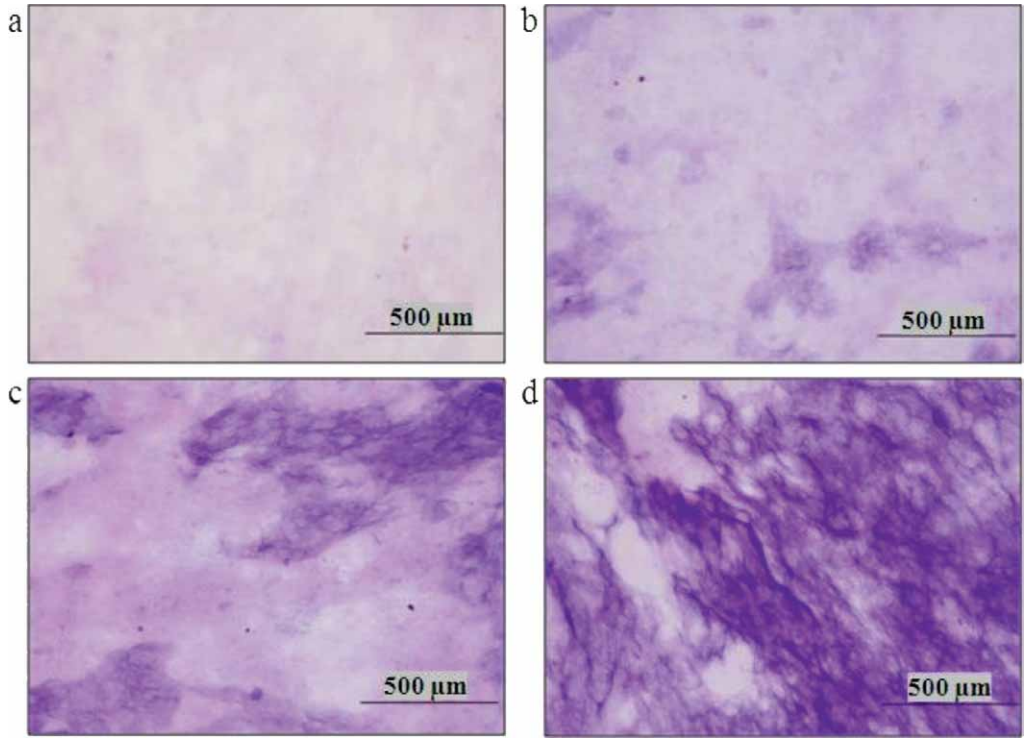

Fig. 3. Optical microscopy with periodic acid-Schiff stain for zein-xanthan biofilms. *w*(xanthan)/%: a) 0 (control), b) 0.01, c) 0.03, and d) 0.04

After optical microscopy analyses, it can be concluded that the observations previously considered as porous on SEM images are in fact fat globules dispersed into the film matrix. Thus it is confirmed that xanthan addition improves homogenization of the compounds mainly with respect to the size and distribution of fat globules.

The chemical structure of xanthan gum and a structural model of zein molecule as proposed by Nery *et al.* (*30*) and Argos *et al.* (*31*), shown in Figs. 4 and 5, help to explain which chemical groups are identified by FTIR--ATR analysis.

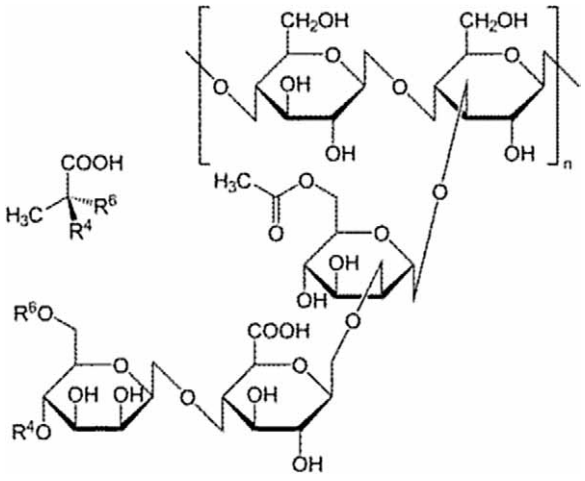

Fig. 4. Chemical model of xanthan gum (*30*)

The spokes in Fig. 5a refer to the amino acid side chain directions in the projected helix. The figure shows three polar regions, each composed of two amino acids. The hydrogen-bonding polar residue segments are shown as small circles in Fig. 5b, in which Up refers to a helical propagation towards the viewer from the NH_2 to COOH terminus while Dn indicates the opposite direction.

Fig. 6 presents the results obtained with FTIR-ATR for all biofilms. The spectra were mathematically treated to correct the base line.

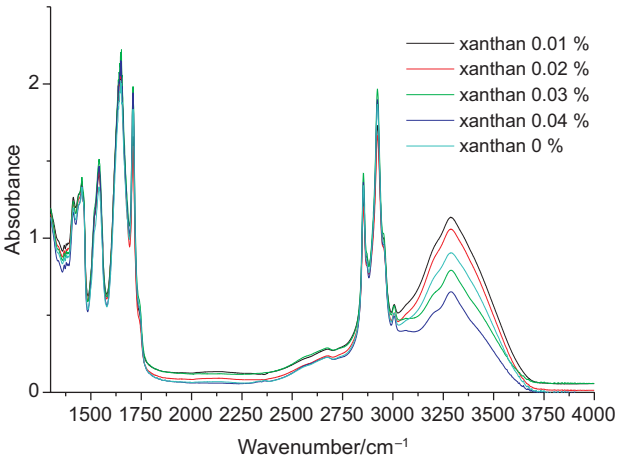

Fig. 6. FTIR-ATR spectra for zein-xanthan biofilms

The internal peaks shown in the spectra of the proteins are mainly due to peptide groups. The proteins in these spectra are characterized as amino group peaks, where amide I at 1650 cm^{-1}, amide II at 1540 cm^{-1} and amide A at 3300 cm^{-1} can be observed. The amide I peak is the evidence of stretching the C=O linkage from peptide groups. Amide II peak refers to stretching of CN linkage as well as the folding of NH group. Amide A characterized as an intense and wide peak represents the stretching of NH group (*32,33*). The peaks of amide I and II in the region between 1500 and 1800 cm^{-1} indicate the predominance of secondary structures α and β (*34,35*).

In the range from 1500 to 3000 cm^{-1}, where no differences were found among the spectra due to xanthan addition, peaks at 1745 cm^{-1} were observed corresponding to carboxyl groups. According to some authors

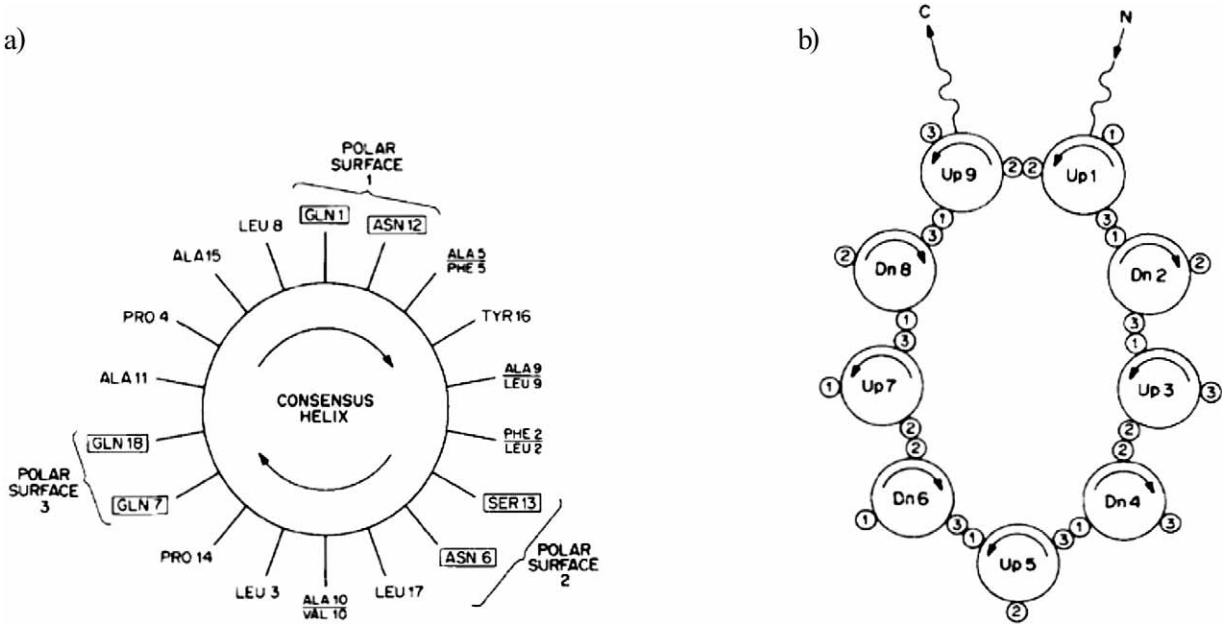

Fig. 5. Structural model of zein molecule: a) helical wheel for 18-residue repeat sequence in Z19 and Z22 zein type, b) a possible nine-helical zein protein structural model. ALA, LEU, *etc.* are initial letters of amino acids. Z19 and Z22 refer to zein with molecular mass of 19 000 and 22 000 Da, respectively. Up refers to a helical propagation towards the viewer from the NH_2 to COOH terminus, while Dn indicates the opposite direction (*31*)

(*34,35*), these groups are probably from free fatty acids. The peaks observed from 2800 to 3100 cm^{-1} indicate CH stretching from functional groups CH_3 and CH_2, also derived from free fatty acids (*36*). These bands appear in the commercial zein, probably due to the higher fat residue in the material as compared to the zein extracted in the laboratory.

The principal evidence of xanthan gum is the band centered at 3300 cm^{-1}, as a consequence of stretching of OH linkages, and the band at 1740 cm^{-1} due to C=O stretching from the esterification with pyruvil (CH-CO--COO) and acetyl (CH-COO), and the glucuronic acid group COOH. The peak at 1640 cm^{-1}, related to angular deformations of the sugar OH linkages, occurs in the same region of amide I and proteins, so the distinction among them is difficult (*32*). The results also indicate the presence of aliphatic compounds (CH) that generate bands with multiple peaks in the region of 2900 to 3000 cm^{-1} (*27,37,38*).

According to Fig. 6, there were great differences in a wide band at 3300 cm^{-1}. This peak corresponds to the combination of two vibrations: the NH group from amide A of the zein and the OH group from xanthan gum. Xanthan addition causes a hypochromic effect in this region, suggesting an interaction between vibrational dipoles from these two groups that causes a decrease of that peak. This effect can be better understood through the correlation spectra, capable of identifying which chemical groups perform the interactions. Figs. 7 and 8 were obtained through bidimensional infrared analysis, whose main characteristic is to attenuate superposition of spectra with transitions (*39–41*).

The 2D synchronous spectrum presents simultaneous changes in intensity spectrum and consists of auto peaks (present in the diagonal line) and cross peaks (located at the off-diagonal position). In a 2D synchronous spectrum, negative cross peaks indicate that the intensity changes observed in two spectral coordinates occur in opposite directions, which means that one increased while the other decreased. A positive cross peak, however, indicates that changes in intensity are in the same direction (*42,43*).

Fig. 7 shows the main peaks along the diagonal. The first peak at 1710 cm^{-1} represents the vibrations of C=O linkages from carboxyl acids, and the other two peaks at 2850 and 2920 cm^{-1} correspond to C-H stretching of zein groups.

The 2D asynchronous spectrum shows the results that occur out of phase with perturbation pulse. This information is manifested in the form of peaks that are always recorded off the diagonal of the bidimensional space (*44,45*).

In the asynchronous spectra (Fig. 8), it is observed that the xanthan addition affects first the C=O linkage of amide I group in the region of 1650 cm^{-1}, and then the functional group N-H of amide II in the region of 1540 cm^{-1}, both from zein, represented by peaks with negative intensity. After these groups had been affected, weak correlations between amides I and II from zein (1650 and 1540 cm^{-1}, respectively) with carboxylic acids (1710 cm^{-1}), and CH_3 (2850 cm^{-1}) and CH_2 (2920 cm^{-1}) from aliphatic compounds also occurred.

The PAS with opacity analyses demonstrates the interference of xanthan in the material transparency. The effects of the addition of xanthan and its concentration on the transparency of the material analyzed by PAS in the UV/VIS and opacity tests are shown in the spectrograms presented in Fig. 9.

The spectra show that in the region of 275 to 350 nm, the increase of xanthan concentration promoted increases in the radiation conversion absorbed as heat. Films with 0 and 0.01 % xanthan presented small peaks in this region. The conversion of maximum radiation occurred at 312 nm.

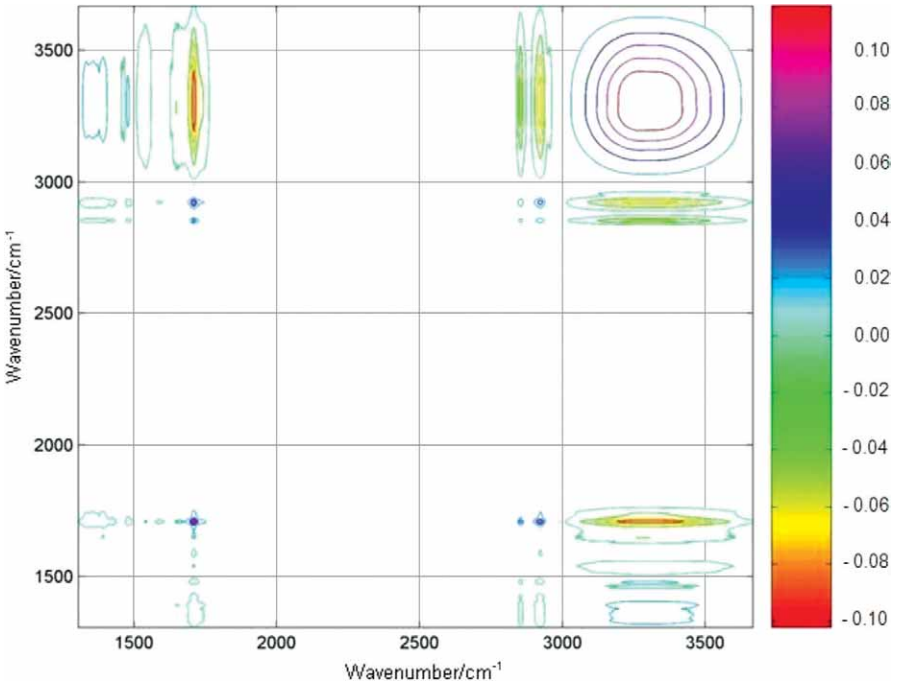

Fig. 7. Synchronous spectra of zein showing functional groups affected by xanthan addition

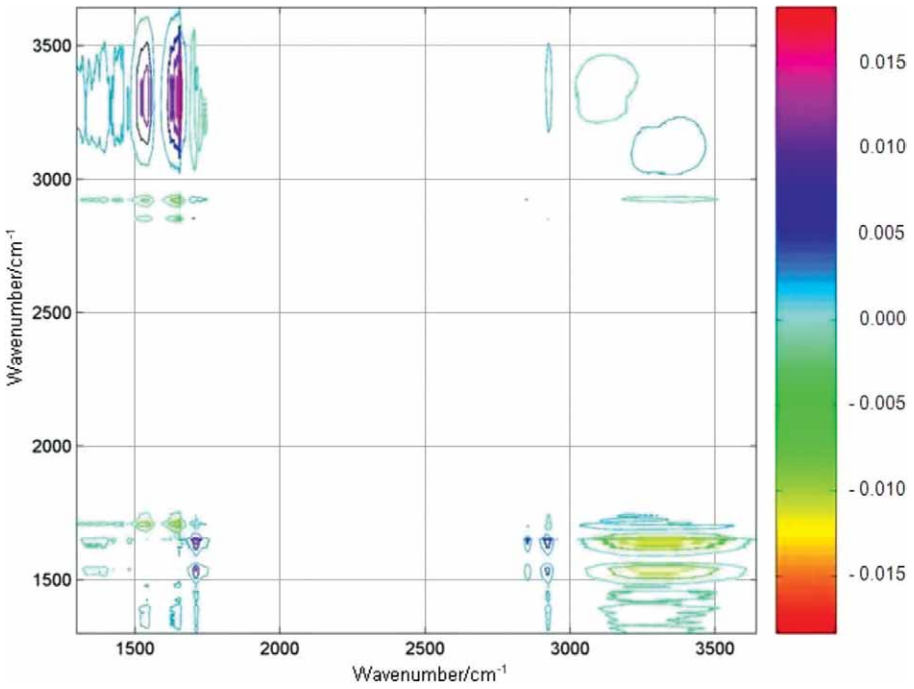

Fig. 8. Asynchronous spectra of zein showing functional groups affected by xanthan addition

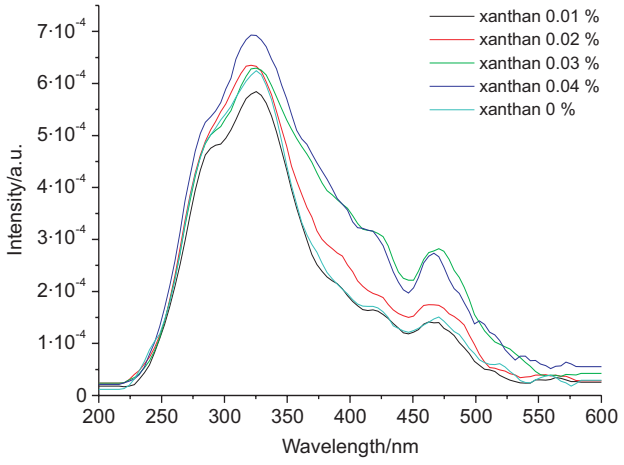

Fig. 9. Photoacoustic spectra of zein-xanthan biofilms

Transparency tests done by UV/VIS spectrometer confirmed the observations of PAS analyses (Table 1). Films with 0.01 % xanthan demonstrated better transparency, or lower opacity, as shown by the peaks with less intensity in the PAS results. Therefore, the addition of xanthan gum in the polymer matrix decreases the transparency of the material.

Table 1. Transparency of the zein-xanthan biofilms obtained by UV/VIS spectrometry

Material	$A_{600\ nm}$	Transparency
zein+sorbitan	0.963±0.04	(7.570±0.29)[b]
zein+xanthan 0.01 %	0.822±0.08	(9.605±0.95)[a]
zein+xanthan 0.02 %	0.811±0.03	(7.277±0.26)[b]
zein+xanthan 0.03 %	0.623±0.09	(7.624±1.13)[b]
zein+xanthan 0.04 %	0.869±0.04	(5.565±0.30)[c]

[a,b,c]Means followed by the same letter in each column are not different according to Tukey´s test ($p<0.05$)

Conclusions

It was possible to produce biofilms composed of zein-xanthan gum. The film prepared with 0.04 % of xanthan was visually less homogeneous due to the presence of lumps across the surface. However, after optical microscopy analysis, it can be concluded that the observations previously considered as pores on SEM images are in fact fat globules dispersed into the film matrix. Thus, it is confirmed that xanthan addition improves homogenization of the compounds, mainly with respect to the size and disposition of the fat globules. Infrared spectroscopy (FTIR-ATR) pointed out that xanthan concentrations deeply affected C=O linkages from amide I group, as well as the functional N-H group of amide II of the zein structure. Other weak correlations of amide I and II with carboxylic acids and aliphatic compounds were also observed. PAS analyses as well transparency measurement by spectrophotometry indicated that xanthan addition to the matrix of the film lowers its transparency properties. Overall, the addition of xanthan gum favoured lipid dispersion in the matrix, making the biofilms more homogeneous, although less transparent.

Acknowledgements

The authors are grateful for financial support provided by FAPESP (São Paulo Research Agency) with grants nos. 2005/02407-4 and 2006/01775-2. C.B.A. thanks CAPES Brazilian agency for fellowship.

References

1. N. Cao, Y. Fu, J. He, Preparation and physical properties of soy proteins isolate and gelatin composite films, *Food Hydrocolloids, 21* (2007) 1153–1162.
2. A. Esen, A proposed nomenclature for the alcohol-soluble proteins (zeins) of maize (*Zea mays* L.), *J. Cereal Sci. 5* (1987) 117–128.
3. R. Regina, O. Solferini, Production of cultivars of ingredients with high nutritional value: characteristics and benefits, *Proceedings of the Symposium on Ingredients in Animal Feed*, Uberlândia, MG, Brazil (2002) pp. 105–116 (in Portuguese).
4. B.A. McGowan, S.Y. Lee, Comparison of methods to analyze time-intensity curves in a corn zein chewing gum study, *Food Qual. Prefer. 17* (2006) 296–306.
5. H.M. Lai, G.W. Padua, Properties and microstructure of plasticized zein films, *Cereal Chem. 74* (1997) 771–775.
6. A.N. Moreira, F.A.B. Del Pino, C.T. Vendruscolo, Study on the biopolymer production by enzymatic pathway through cellular inactivation and lyse and with viable cells by *Beijerinckia* sp. 7070, *Ciênc. Tecnol. Aliment. 23* (2003) 300–305 (in Portuguese).
7. F.M. Maugeri Filho: Production of Polysaccharides. In: *Biotecnologia Industrial, Vol. 3*, U.A. Lima, E. Aquarone, W. Borzani, W. Schmidell (Eds.), Editora Edgar Blucher Ltd, São Paulo, Brazil (2001) p. 593 (in Portuguese).
8. E.R. Morris: Polysaccharide Rheology and In-Mouth Perception. In: *Food Polysaccharides and Their Applications*, A.M. Stephen (Ed.), Marcel Dekker, New York, USA (1995) pp. 517–546.
9. N. Lagoueyte, P. Paquin, Effects of microfluidization on the functional properties of xanthan gums, *Food Hydrocolloids, 12* (1998) 365–371.
10. H.M. Lai, G.W. Padua, Water vapor barrier properties of zein films plasticized with oleic acid, *Cereal Chem. 75* (1998) 194–199.
11. K. Yamada, H. Takahashi, A. Noguchi, Improved water resistance in edible zein films and composites for biodegradable food packaging, *Int. J. Food Sci. Technol. 30* (1995) 599–608.
12. H.J. Park, M.S. Chinnan, Gas and water vapor barrier properties of edible films from protein and cellulosic materials, *J. Food Eng. 25* (1995) 497–507.
13. T. Ohnaga, T. Sato, S. Nagata, Miscibility and phase-behavior of methyl-methacrylate copolymer and polycarbonate blends, *Polymer, 38* (1997) 1073–1079.
14. D.T.D.F. Rosa, Optical and thermal characterization of polymeric materials by photothermal methods, *PhD Thesis*, University of Maringá, Maringá, Brazil (2005) (in Portuguese).
15. D.R. Paul, S. Newman: *Polymer Blends, Vol. 2*, Academic Press, New York, USA (1978).
16. E. Da Costa Mattos, I. Vigano, R.C.L. Dutra, Application of FTIR methodologies of transmission and photoacoustic to the characterization of highly energetic materials: Part II, *Quím. Nova, 25* (2002) 722–728 (in Portuguese).
17. C.F. Pereira, C. Pasquini, Two-dimensional correlation spectroscopy: Fundamentals, applications and perspectives, *Quím. Nova, 29* (2006) 143–148 (in Portuguese).
18. L. Yang, A.T. Paulson, Effects of lipids on mechanical and moisture barrier properties of edible gellan film, *Food Res. Int. 33* (2000) 571–578.
19. D. Kleen, G. Padua, N. Engeseth, Stabilization of lipids in a biodegradable zein-oleate film by incorporation of antioxidants, *Cereal Chem. 79* (2002) 687–694.
20. L.A. Forato, Study of structures of zein by NMR, FTIR and MFA, *PhD Thesis*, University of São Paulo, São Paulo, Brazil (2000) (in Portuguese).
21. B.C. Vidal, Dichroism in collagen bundles stained with Xylidine-Ponceau 2R, *Ann. Histochim. 15* (1970) 289–296.
22. A.G.E. Pearse: *Histochemistry, Theoretical and Applied: Preparative and Optical Technology, Vol. 1*, Churchill Livingstone, Edinburgh, UK (1980) 439.
23. D.M.R. Georget, S.A. Barker, P.S. Belton, A study on maize proteins as a potential new tablet excipient, *Eur. J. Pharm. Biopharm. 69* (2008) 718–726.
24. M.R. Bugs, R.K. Bortoleto-Bugs, M. Lopes Cornélio, Photoacoustic spectroscopy of aromatic amino acids proteins, *Eur. Biophys. J. 37* (2008) 205–212.
25. M.E. Gounga, S.Y. Xu, Z. Wang, Whey protein isolate-based edible films as affected by protein concentration, glycerol ratio and pullulan addition in film formation, *J. Food Eng. 83* (2007) 521–530.
26. D.A. Banzatto, S.N. Kronka: *Agricultural Experimentation*, FUNEP, Jaboticabal, Brazil (2006) (in Portuguese).
27. E. Corradini, Development of polymeric blends of corn starch and zein, *PhD Thesis*, University of São Paulo, São Carlos, Brazil (2004) (in Portuguese).
28. B. Ghanbarzadeh, M. Musavi, A.R. Oromiehie, K. Rezayi, E.R. Rad, J. Milani, Effect of plasticizing sugars on water vapor permeability, surface energy and microstructure properties of zein films, *LWT-Food Sci. Technol. 40* (2007) 1191–1197.
29. J.D. Bancroft, A. Stevens: *Theory and Practice of Histological Techniques*, Churchill Livingstone, Edinburgh, UK (1990) pp. 187–189.
30. T.B.R. Nery, L.V. Brandão, M.C.A. Esperidião, J.I. Druzian, Biosynthesis of xanthan gum from the fermentation of milk whey: Productivity and viscosity, *Quím. Nova, 31* (2008) 1937–1941 (in Portuguese).
31. P. Argos, K. Pedersen, M.D. Marks, B.A. Larkins, A structural model for maize zein proteins, *J. Biol. Chem. 257* (1982) 9984–9990.
32. D. Osiro, H.D. Della Coletta Filho, M.A. Machado, L.A. Colnago, Use of FTIR for the analysis of bacteria that cause citrus cancer and CVC, *EMBRAPA Technical Report, 40*, EMBRAPA, São Carlos, Brazil (2000) pp. 1–5 (in Portuguese).
33. D. Osiro, L.A. Colnago, A.M.M.B. Otoboni, E.G.M. Lemos, A.A. de Souza, H.D. Della Coletta Filho, M.A. Machado, A kinetic model for *Xylella fastidiosa* adhesion, biofilm formation, and virulence, *FEMS Microbiol. Lett. 236* (2004) 313–318.
34. L.A. Forato, R. Bernardes-Filho, L.A. Colnago, Protein structure in KBr pellets by infrared spectroscopy, *Anal. Biochem. 259* (1998) 136–141.
35. L. Marcotte, G. Kegelaer, C. Sandt, J. Barbeau, M. Lafleur, An alternative infrared spectroscopy assay for the quantification of polysaccharides in bacterial samples, *Anal. Biochem. 361* (2007) 17–47.
36. L.A. Forato, T.C. Bicudo, L.A. Colnago, Conformation of α zeins in solid state by Fourier transform IR, *Biopolymers, 72* (2003) 421–426.
37. L.A. Forato, V.E. Yushmanov, L.A. Colnago, Interaction of two prolamins with 1–^{13}C oleic acid by ^{13}C NMR, *Biochemistry, 43* (2004) 7121–7126.
38. D.M.R. Georget, S.A. Barker, P.S. Belton, A study on maize proteins as a potential new tablet excipient, *Eur. J. Pharm. Biopharm. 69* (2008) 718–726.
39. R.M. Silverstein, G.C. Bassler, T.C. Morril: *Spectrometric Identification of Organic Compounds*, John Wiley & Sons, New York, USA (1974) p. 424.

40. J.A. Scramin, D. Britto, O.B.G. Assis, L.A. Colnago, L.A. Forato, Surface wetting and DMA characterization of zein/oleic acid based films, *Proceedings of the XI International Macromolecular Colloquium and 6th ISNAPOL*, Gramado, Brazil (2007).

41. I. Noda, A.E. Dowrey, C. Marcoli, G.M. Story, Y. Ozaki, Generalized two-dimensional correlation spectroscopy, *Appl. Spectrosc. 54* (2000) 236A–248A.

42. I. Noda, Two-dimensional infrared (2D IR) spectroscopy: Theory and applications, *Appl. Spectrosc. 44* (1990) 550–561.

43. I. Noda, Generalized two-dimensional correlation method applicable to infrared, raman, and other types of spectroscopy, *Appl. Spectrosc. 47* (1993) 1329–1336.

44. D.A. Skoog, F.J. Holler, T.A. Nieman: *Principles of Instrumental Analysis*, Thomson Learning, USA (2002) p. 434.

45. H. Fabian, H.H. Mantsch, C.P. Shultz, Two-dimensional IR correlation spectroscopy: Sequential events in the unfolding process of the λ Cro-V55C repressor protein, *PNAS*, *96* (1999) 13153–13158.